

# Chiral Phase Transition in 3-flavor QCD from Lattice QCD

Sipaz Sharma

in collaboration with

L.Dini, P.Hegde, F.Karsch, A.Lahiri, C.Schmidt

March 30, 2022

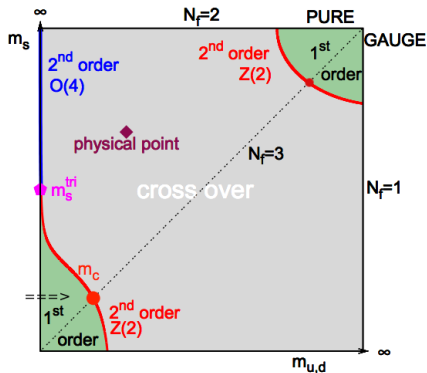


# Outline

- ▶ Motivation : Pisarski and Wilczek remarks.
- ▶ Past Work.
- ▶ Universal properties near a critical point.
- ▶ Definitions of chiral observables and simulation details.
- ▶ Results for order parameter and its susceptibility.
- ▶ Finite size scaling analysis.
- ▶ Conclusions & Outlook.

# Motivation

$$\blacktriangleright SU(N_f)_L \times SU(N_f)_R \rightarrow SU(N_f)_V$$



- $\blacktriangleright$  In the chiral limit the order of the QCD phase transition depends on the number of quark flavours that become massless. For  $N_f \geq 3$  massless quark flavors, this phase transition is first order.

[Pisarski & Wilczek, 1983]

Figure: Columbia Plot  
[A.Peikert, Ph.D. Thesis, 2000]

# Past work

- ▶ For calculations performed with unimproved gauge and fermion actions, bounds on the critical parameters show a strong cut-off and discretization dependence.

[F.Karsch et al., 2001] [Philippe de Forcrand et al., 2016]

# Past work

- ▶ For calculations performed with unimproved gauge and fermion actions, bounds on the critical parameters show a strong cut-off and discretization dependence.  
[F.Karsch et al., 2001] [Philippe de Forcrand et al., 2016]
- ▶ Calculations were performed using HISQ action on  $N_\tau = 6$  lattices. No direct evidence of a first order region was found. An upper bound for the critical pion mass was estimated to be equal to 50 MeV.  
[A. Bazavov et al., 2017]

# Past work

- ▶ For calculations performed with unimproved gauge and fermion actions, bounds on the critical parameters show a strong cut-off and discretization dependence.  
[F.Karsch et al., 2001] [Philippe de Forcrand et al., 2016]
- ▶ Calculations were performed using HISQ action on  $N_\tau = 6$  lattices. No direct evidence of a first order region was found. An upper bound for the critical pion mass was estimated to be equal to 50 MeV.  
[A. Bazavov et al., 2017]
- ▶ Wilson-Clover fermion action was used to put an upper bound on critical pion mass which was found to be equal to 110 MeV.  $T_E$  was quoted to be equal to 134(3) MeV.  
[Y. Kuramashi et al., 2020]

# Universal properties near a critical point

- ▶ In the vicinity of a second order critical point, singular part of the free energy density dominates.

$$f_s(t, h, \dots) = b^{-d} f_s(b^{y_t} t, b^{y_h} h, \dots)$$

[J. Engels et al., 2000] [Ejiri, Karsch et al., 2009]

# Universal properties near a critical point

- ▶ In the vicinity of a second order critical point, singular part of the free energy density dominates.

$$f_s(t, h, \dots) = b^{-d} f_s(b^{y_t} t, b^{y_h} h, \dots)$$

[J. Engels et al., 2000] [Ejiri, Karsch et al., 2009]

- ▶  $t$  and  $h$  are the reduced scaling variables :

$$t = \frac{1}{t_0} \frac{T - T_c}{T_c}, \quad h = \frac{H}{h_0}; \quad t_0, h_0 \text{ are non universal parameters.}$$

# Universal properties near a critical point

- ▶ In the vicinity of a second order critical point, singular part of the free energy density dominates.

$$f_s(t, h, \dots) = b^{-d} f_s(b^{y_t} t, b^{y_h} h, \dots)$$

[J. Engels et al., 2000] [Ejiri, Karsch et al., 2009]

- ▶  $t$  and  $h$  are the reduced scaling variables :

$$t = \frac{1}{t_0} \frac{T - T_c}{T_c}, \quad h = \frac{H}{h_0}; \quad t_0, h_0 \text{ are non universal parameters.}$$

- ▶  $b$  can be chosen such that  $f_s$  becomes function of one argument :

$$f_s(t, h) = h^{1+1/\delta} f_s(z, 1), \quad z = t/h^{1/\beta\delta}$$

# Universal properties near a critical point

- ▶ In the vicinity of a second order critical point, singular part of the free energy density dominates.

$$f_s(t, h, \dots) = b^{-d} f_s(b^{y_t} t, b^{y_h} h, \dots)$$

[J. Engels et al., 2000] [Ejiri, Karsch et al., 2009]

- ▶  $t$  and  $h$  are the reduced scaling variables :

$$t = \frac{1}{t_0} \frac{T - T_c}{T_c}, \quad h = \frac{H}{h_0}; \quad t_0, h_0 \text{ are non universal parameters.}$$

- ▶  $b$  can be chosen such that  $f_s$  becomes function of one argument :

$$f_s(t, h) = h^{1+1/\delta} f_s(z, 1), \quad z = t/h^{1/\beta\delta}$$

- ▶  $O(2)$  &  $Z(2)$  will have different critical exponents.

# Universal properties near a critical point

- ▶ In the vicinity of a second order critical point, singular part of the free energy density dominates.

$$f_s(t, h, \dots) = b^{-d} f_s(b^{y_t} t, b^{y_h} h, \dots)$$

[J. Engels et al., 2000] [Ejiri, Karsch et al., 2009]

- ▶  $t$  and  $h$  are the reduced scaling variables :

$$t = \frac{1}{t_0} \frac{T - T_c}{T_c}, \quad h = \frac{H}{h_0}; \quad t_0, h_0 \text{ are non universal parameters.}$$

- ▶  $b$  can be chosen such that  $f_s$  becomes function of one argument :

$$f_s(t, h) = h^{1+1/\delta} f_s(z, 1), \quad z = t/h^{1/\beta\delta}$$

- ▶  $O(2)$  &  $Z(2)$  will have different critical exponents.
- ▶ For  $Z(2)$ ,  $H \rightarrow H - H_c$ .

# Universal properties near a critical point

- ▶ In the vicinity of a second order critical point, singular part of the free energy density dominates.

$$f_s(t, h, \dots) = b^{-d} f_s(b^{y_t} t, b^{y_h} h, \dots)$$

[J. Engels et al., 2000] [Ejiri, Karsch et al., 2009]

- ▶  $t$  and  $h$  are the reduced scaling variables :

$$t = \frac{1}{t_0} \frac{T - T_c}{T_c}, \quad h = \frac{H}{h_0}; \quad t_0, h_0 \text{ are non universal parameters.}$$

- ▶  $b$  can be chosen such that  $f_s$  becomes function of one argument :

$$f_s(t, h) = h^{1+1/\delta} f_s(z, 1), \quad z = t/h^{1/\beta\delta}$$

- ▶  $O(2)$  &  $Z(2)$  will have different critical exponents.
- ▶ For  $Z(2)$ ,  $H \rightarrow H - H_c$ .
- ▶ No evidence of a first order region, therefore, only  $O(2)$  scaling functions have been used in the analysis.

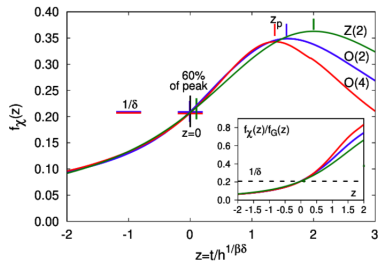
# Universal properties near a critical point

$$M = -\frac{\partial f_s(t, h)}{\partial H} = h^{1/\delta} f_G(z)$$

$$\chi_M = \frac{\partial M}{\partial H} = \frac{1}{h_0} h^{1/\delta-1} f_\chi(z)$$

$$\frac{f_\chi(z)}{f_G(z)} = \frac{1}{\delta} \left( 1 - \frac{z f'_G(z)}{\beta f_G(z)} \right)$$

- ▶  $f_\chi(z)$  peaks at  $z_p$ , which is a characteristic value for a given theory.



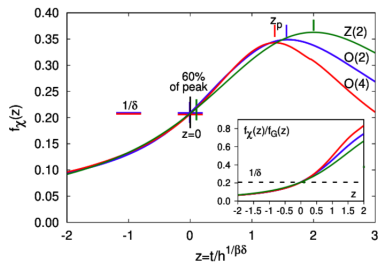
[H.-T. Ding et al., 2019]

# Universal properties near a critical point

$$M = -\frac{\partial f_s(t, h)}{\partial H} = h^{1/\delta} f_G(z)$$

$$\chi_M = \frac{\partial M}{\partial H} = \frac{1}{h_0} h^{1/\delta-1} f_\chi(z)$$

$$\frac{f_\chi(z)}{f_G(z)} = \frac{1}{\delta} \left( 1 - \frac{z f'_G(z)}{\beta f_G(z)} \right)$$



[H.-T. Ding et al., 2019]

- ▶  $f_\chi(z)$  peaks at  $z_p$ , which is a characteristic value for a given theory.
- ▶  $f_\chi/f_G$  has a unique crossing point at  $z = 0$ .

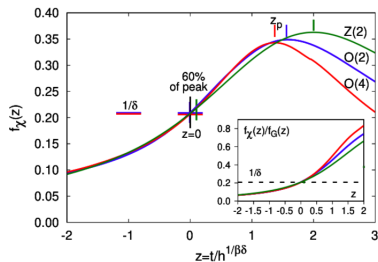
# Universal properties near a critical point

$$M = -\frac{\partial f_s(t, h)}{\partial H} = h^{1/\delta} f_G(z)$$

$$\chi_M = \frac{\partial M}{\partial H} = \frac{1}{h_0} h^{1/\delta-1} f_\chi(z)$$

$$\frac{f_\chi(z)}{f_G(z)} = \frac{1}{\delta} \left( 1 - \frac{z f'_G(z)}{\beta f_G(z)} \right)$$

- ▶  $f_\chi(z)$  peaks at  $z_p$ , which is a characteristic value for a given theory.
- ▶  $f_\chi/f_G$  has a unique crossing point at  $z = 0$ .
- ▶  $M - H\chi_M$  does not receive regular contribution at  $\mathcal{O}(H)$ .



[H.-T. Ding et al., 2019]

# Chiral Observables

- ▶ Partition function of QCD with  $N_f$  degenerate quark flavors :

$$\mathcal{Z} = \int \mathcal{D}[U] \{ \det D(m_\ell) \}^{N_f/4} e^{-S_g}$$

# Chiral Observables

- ▶ Partition function of QCD with  $N_f$  degenerate quark flavors :

$$\mathcal{Z} = \int \mathcal{D}[U] \{ \det D(m_\ell) \}^{N_f/4} e^{-S_g}$$



$$\frac{1}{\mathcal{Z}} \frac{\partial \mathcal{Z}}{\partial m_\ell} = \frac{N_f}{4} \langle \text{tr}(D^{-1}) \rangle = N_\sigma^3 N_\tau \langle \bar{\psi} \psi \rangle \rightarrow M$$

$1/4$  is the staggered rooting factor,  $N_\tau = (aT)^{-1}$ , and  $V = (aN_\sigma)^3$

# Chiral Observables

- ▶ Partition function of QCD with  $N_f$  degenerate quark flavors :

$$\mathcal{Z} = \int \mathcal{D}[U] \{ \det D(m_\ell) \}^{N_f/4} e^{-S_g}$$



$$\frac{1}{\mathcal{Z}} \frac{\partial \mathcal{Z}}{\partial m_\ell} = \frac{N_f}{4} \langle \text{tr}(D^{-1}) \rangle = N_\sigma^3 N_\tau \langle \bar{\psi} \psi \rangle \rightarrow M$$



$$\begin{aligned} \frac{\partial \langle \bar{\psi} \psi \rangle}{\partial m_\ell} &= \frac{N_f^2}{16 N_\sigma^3 N_\tau} \underbrace{\left[ \langle (\text{tr} D^{-1})^2 \rangle - \langle \text{tr} D^{-1} \rangle^2 \right]}_{\chi_{\text{disc}}} \\ &\quad - \underbrace{\frac{N_f}{4 N_\sigma^3 N_\tau} \langle \text{tr}(D^{-2}) \rangle}_{\chi_{\text{con}}} = \chi_{\text{tot}} \rightarrow \chi_M \end{aligned}$$

# Chiral Observables

- ▶ Partition function of QCD with  $N_f$  degenerate quark flavors :

$$\mathcal{Z} = \int \mathcal{D}[U] \{ \det D(m_\ell) \}^{N_f/4} e^{-S_g}$$



$$\frac{1}{\mathcal{Z}} \frac{\partial \mathcal{Z}}{\partial m_\ell} = \frac{N_f}{4} \langle \text{tr}(D^{-1}) \rangle = N_\sigma^3 N_\tau \langle \bar{\psi} \psi \rangle \rightarrow M$$



$$\begin{aligned} \frac{\partial \langle \bar{\psi} \psi \rangle}{\partial m_\ell} &= \underbrace{\frac{N_f^2}{16 N_\sigma^3 N_\tau} \left[ \langle (\text{tr} D^{-1})^2 \rangle - \langle \text{tr} D^{-1} \rangle^2 \right]}_{\chi_{\text{disc}}} \\ &\quad - \underbrace{\frac{N_f}{4 N_\sigma^3 N_\tau} \langle \text{tr}(D^{-2}) \rangle}_{\chi_{\text{con}}} = \chi_{\text{tot}} \rightarrow \chi_M \end{aligned}$$

- ▶  $H \rightarrow m_\ell/m_s$  ,  $T \rightarrow T$

$m_s$  is an external parameter used to set scale for  $m_\ell$ .

## Simulation details

- ▶ For the HISQ/tree action calculations, Bielefeld GPU code has been used.

# Simulation details

- ▶ For the HISQ/tree action calculations, Bielefeld GPU code has been used.
- ▶  $N_\tau$  value was fixed to be equal to 8 and three different aspect ratios ( $N_\sigma/N_\tau$ ) : 5,4,3 were explored.

# Simulation details

- ▶ For the HISQ/tree action calculations, Bielefeld GPU code has been used.
- ▶  $N_\tau$  value was fixed to be equal to 8 and three different aspect ratios ( $N_\sigma/N_\tau$ ) : 5,4,3 were explored.
- ▶  $f_K$  scale setting from 2+1 flavor was used to fix the temperatures for various values of gauge couplings as well as quark masses ( $m_\ell$ ), which are relative to the LCP for 2+1 flavor, which corresponds to physical strange quark mass ( $m_s$ ). [A.Bazavov et al., 2012]

# Simulation details

- ▶ For the HISQ/tree action calculations, Bielefeld GPU code has been used.
- ▶  $N_\tau$  value was fixed to be equal to 8 and three different aspect ratios ( $N_\sigma/N_\tau$ ) : 5,4,3 were explored.
- ▶  $f_K$  scale setting from 2+1 flavor was used to fix the temperatures for various values of gauge couplings as well as quark masses ( $m_\ell$ ), which are relative to the LCP for 2+1 flavor, which corresponds to physical strange quark mass ( $m_s$ ). [A.Bazavov et al., 2012]
- ▶ Four quark masses were investigated, which in the continuum correspond to pion masses in the range 80 MeV to 140 MeV.

# Simulation details

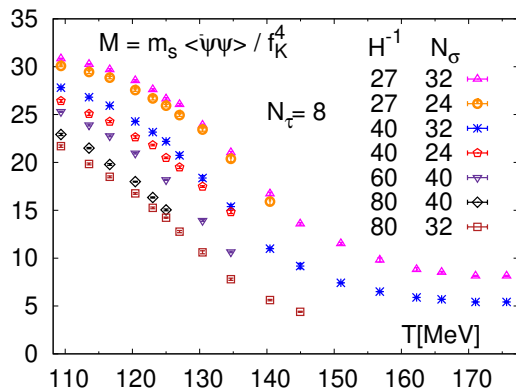
- ▶ For the HISQ/tree action calculations, Bielefeld GPU code has been used.
- ▶  $N_\tau$  value was fixed to be equal to 8 and three different aspect ratios ( $N_\sigma/N_\tau$ ) : 5,4,3 were explored.
- ▶  $f_K$  scale setting from 2+1 flavor was used to fix the temperatures for various values of gauge couplings as well as quark masses ( $m_\ell$ ), which are relative to the LCP for 2+1 flavor, which corresponds to physical strange quark mass ( $m_s$ ). [A.Bazavov et al., 2012]
- ▶ Four quark masses were investigated, which in the continuum correspond to pion masses in the range 80 MeV to 140 MeV.
- ▶ Every trajectory separated by 5 TU was saved. 100 random vectors were used for calculating fermionic observables.

# Simulation details

- ▶ For the HISQ/tree action calculations, Bielefeld GPU code has been used.
- ▶  $N_\tau$  value was fixed to be equal to 8 and three different aspect ratios ( $N_\sigma/N_\tau$ ) : 5,4,3 were explored.
- ▶  $f_K$  scale setting from 2+1 flavor was used to fix the temperatures for various values of gauge couplings as well as quark masses ( $m_\ell$ ), which are relative to the LCP for 2+1 flavor, which corresponds to physical strange quark mass ( $m_s$ ). [A.Bazavov et al., 2012]
- ▶ Four quark masses were investigated, which in the continuum correspond to pion masses in the range 80 MeV to 140 MeV.
- ▶ Every trajectory separated by 5 TU was saved. 100 random vectors were used for calculating fermionic observables.
- ▶ Number of saved trajectories:

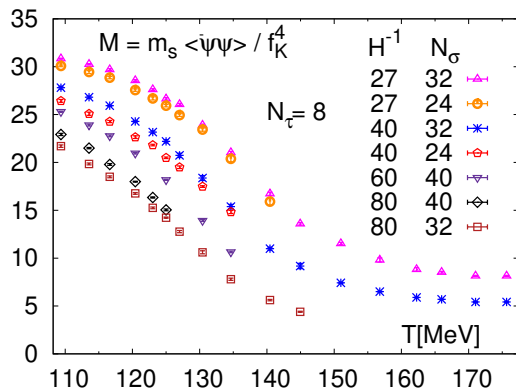
$m_s/m_\ell$	27	40	60	80
	O(1000)	O(1000)	O(3500)	O(5000)

# Chiral condensate in $f_K$ normalization



Similar to  $m_s$ ,  $f_K$  is an external parameter used to set scale for T.

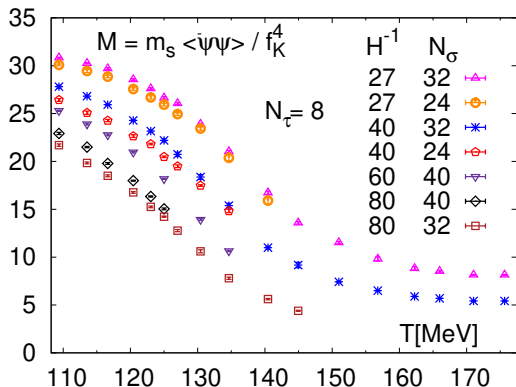
# Chiral condensate in $f_K$ normalization



- Order parameter varies rapidly, but smoothly with the temperature.

Similar to  $m_s$ ,  $f_K$  is an external parameter used to set scale for  $T$ .

# Chiral condensate in $f_K$ normalization

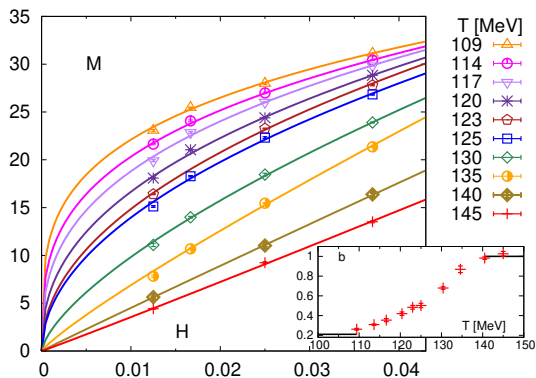


Similar to  $m_s$ ,  $f_K$  is an external parameter used to set scale for  $T$ .

- ▶ Order parameter varies rapidly, but smoothly with the temperature.
- ▶ In the lower temperature region, as the quark mass decreases, finite size effects increase.

# Order parameter at fixed T

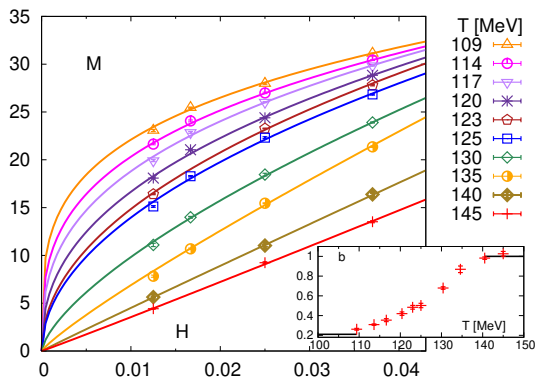
$$M = h^{1/\delta} f_G(z) + H \left\{ a_0 + a_1 \left( \frac{T - T_c}{T_c} \right) + a_2 \left( \frac{T - T_c}{T_c} \right)^2 + \dots \right\} + \dots$$



► Fit ansatz,  $aH^b$ .

# Order parameter at fixed T

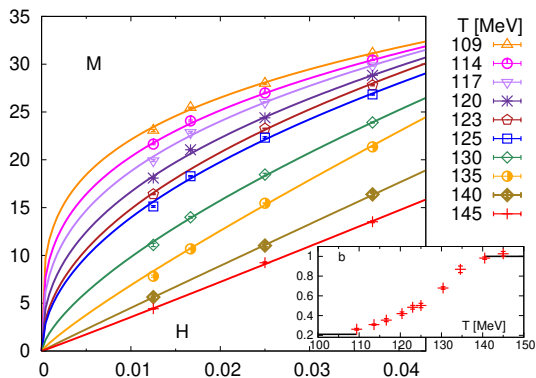
$$M = h^{1/\delta} f_G(z) + H \left\{ a_0 + a_1 \left( \frac{T - T_c}{T_c} \right) + a_2 \left( \frac{T - T_c}{T_c} \right)^2 + \dots \right\} + \dots$$



- Fit ansatz,  $aH^b$ .
- At high temperatures,  $M$  is linear in  $H$ .

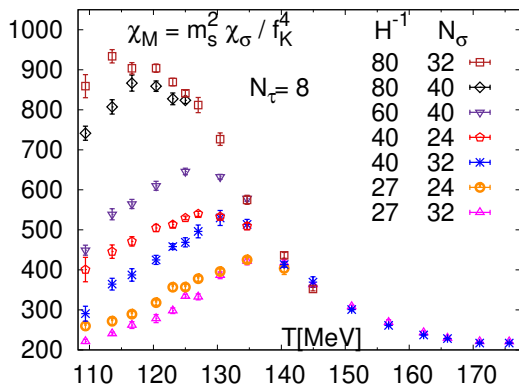
# Order parameter at fixed T

$$M = h^{1/\delta} f_G(z) + H \left\{ a_0 + a_1 \left( \frac{T - T_c}{T_c} \right) + a_2 \left( \frac{T - T_c}{T_c} \right)^2 + \dots \right\} + \dots$$



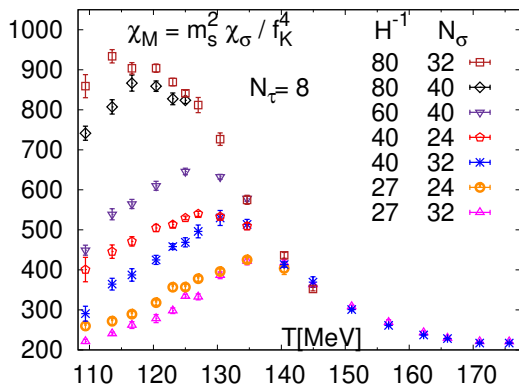
- Fit ansatz,  $aH^b$ .
- At high temperatures, M is linear in H.
- At the lowest T, b is slightly greater than the critical exponent of the 3-d  $O(2)$  universality class. We have bracketed the scaling window.

# Total susceptibility in $f_K$ normalization



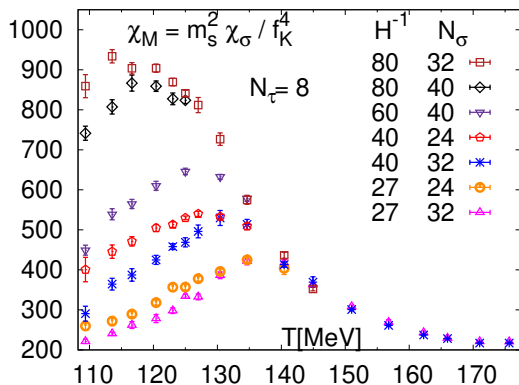
▶ Consistent with  
 $t_p(h) = z_p h^{1/\beta\delta}$ .

# Total susceptibility in $f_K$ normalization



- ▶ Consistent with  $t_p(h) = z_p h^{1/\beta\delta}$ .
- ▶ Peak height for a fixed mass doesn't increase with the volume. No evidence of a first order transition.

# Total susceptibility in $f_K$ normalization



- ▶ Consistent with  $t_p(h) = z_p h^{1/\beta\delta}$ .
- ▶ Peak height for a fixed mass doesn't increase with the volume. No evidence of a first order transition.
- ▶ Peak gets less resolved for the lowest volume of the lowest quark mass. Finite-size effects need to be accounted for.

# Finite size dependence of scaling functions

- ▶ One additional relevant scaling field  $\ell = L_0/L$  can be added to the singular part of the free energy density :

$$f_s(t, h, \ell, \dots) = b^{-d} f_s(b^{y_t} t, b^{y_h} h, b\ell \dots)$$

[Engels & Karsch, 2014]

# Finite size dependence of scaling functions

- ▶ One additional relevant scaling field  $\ell = L_0/L$  can be added to the singular part of the free energy density :

$$f_s(t, h, \ell, \dots) = b^{-d} f_s(b^{y_t} t, b^{y_h} h, b\ell \dots)$$

[Engels & Karsch, 2014]

- ▶  $f_s$  can be brought to a form such that it depends upon two scaling variables,  $z = t/h^{1/\beta\delta}$  and  $z_L = \ell/h^{\nu/\beta\delta}$

$$M = -\frac{\partial f_s}{\partial H} = h^{1/\delta} f_G(z, z_L) + H \times \text{reg}$$

$$\chi_M = \frac{\partial M}{\partial H} = \frac{1}{h_0} h^{1/\delta-1} f_\chi(z, z_L) + \text{reg}$$

$$\text{reg} = a_0 + a_1(t t_0) + a_2(t t_0)^2$$

# Finite size dependence of scaling functions

- ▶ One additional relevant scaling field  $\ell = L_0/L$  can be added to the singular part of the free energy density :

$$f_s(t, h, \ell, \dots) = b^{-d} f_s(b^{y_t} t, b^{y_h} h, b \ell, \dots)$$

[Engels & Karsch, 2014]

- ▶  $f_s$  can be brought to a form such that it depends upon two scaling variables,  $z = t/h^{1/\beta\delta}$  and  $z_L = \ell/h^{\nu/\beta\delta}$

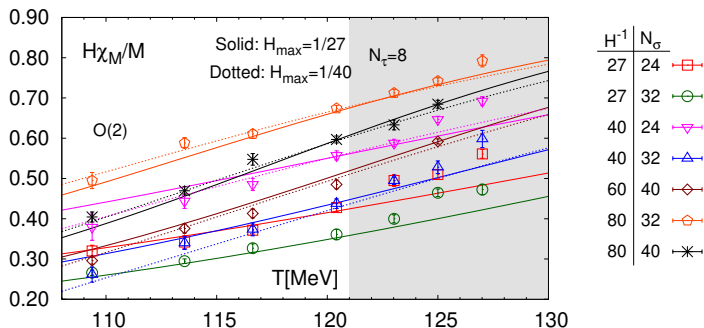
$$M = -\frac{\partial f_s}{\partial H} = h^{1/\delta} f_G(z, z_L) + H \times \text{reg}$$

$$\chi_M = \frac{\partial M}{\partial H} = \frac{1}{h_0} h^{1/\delta-1} f_\chi(z, z_L) + \text{reg}$$

$$\text{reg} = a_0 + a_1(t t_0) + a_2(t t_0)^2$$

- ▶ We used finite size scaling functions to fit data corresponding to quantities such as  $H\chi_M/M$  and  $M - H\chi_M$  for various available combinations of quark masses and volumes.  $T_c$  can be extracted as a fit parameter.

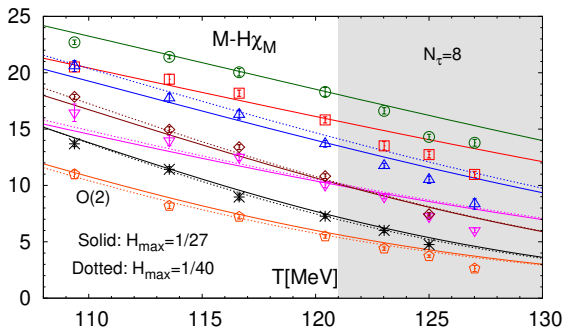
# Joint fit to $H\chi_M/M$ (Ratio)



$H_{\max}^{-1}$	27	40
$T_c$ [MeV]	101(2)	93(4)
$\chi^2/\text{dof}$	2.97	1.32

- ▶ Grey region is not included in the fit.
- ▶ Ratio should have a unique crossing point in the thermodynamic limit, which in this case is below the temperature range explored and gets spoiled by the regular contribution (Linear in  $t t_0$ ).

# Joint fit to $M - H\chi_M$ (Difference)



$H_{\max}^{-1}$	$N_{\sigma}$	Symbol
27	24	Red square
27	32	Green circle
40	24	Magenta inverted triangle
40	32	Blue triangle
60	40	Brown diamond
80	32	Orange square
80	40	Black asterisk

$H_{\max}^{-1}$	27	40
$T_c$ [MeV]	100(1)	97(1)
$\chi^2/\text{dof}$	4.52	2.44

- ▶ Grey region is not included in the fit.
- ▶ This quantity scales as  $\mathcal{O}(H)^3$  at high temperatures.

# Comparison of the fits results

- ▶ The parameters of the singular part of the fits from both the quantities are in excellent agreement with each other.

# Comparison of the fits results

- ▶ The parameters of the singular part of the fits from both the quantities are in excellent agreement with each other.
- ▶ The parameters of the regular term seem to be quite sensitive to the upper bound ( $H_{\max}$ ) for the set of quark masses used in the fit. They are not well determined in the small temperature interval used for these fits.

## Finite size scaling of $T_{pc}$

- ▶  $T_{pc}$  values correspond to the peak positions of various susceptibility curves. Peak position is a function of mass as well as volume.

# Finite size scaling of $T_{pc}$

- ▶  $T_{pc}$  values correspond to the peak positions of various susceptibility curves. Peak position is a function of mass as well as volume.
- ▶ To extract  $T_{pc}(H, L)$  values, we constructed 100 bootstrap samples at the level of gauge configurations and performed quadratic fits in the peak range for each such sample.

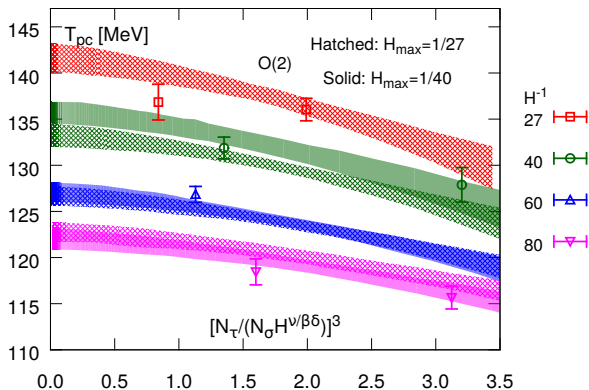
# Finite size scaling of $T_{pc}$

- ▶  $T_{pc}$  values correspond to the peak positions of various susceptibility curves. Peak position is a function of mass as well as volume.
- ▶ To extract  $T_{pc}(H, L)$  values, we constructed 100 bootstrap samples at the level of gauge configurations and performed quadratic fits in the peak range for each such sample.
- ▶  $T_{pc}$  can be fitted to the scaling expectation,

$$T_{pc}(H, L) = T_c \left( 1 + \frac{z_p(z_L)}{z_0} H^{1/\beta\delta} \right)$$

[H.-T. Ding et al., 2019]

# Finite size scaling of $T_{pc}$

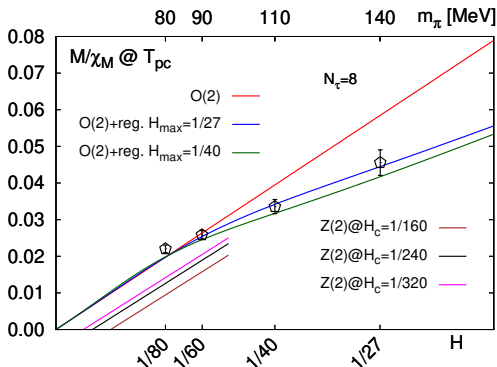


$$T_{pc}(H, L) = T_c \left( 1 + \frac{z_p(z_L)}{z_0} H^{1/\beta\delta} \right)$$

$$[N_\tau / N_\sigma H^\nu / \beta\delta]^3 \propto z_L^3.$$

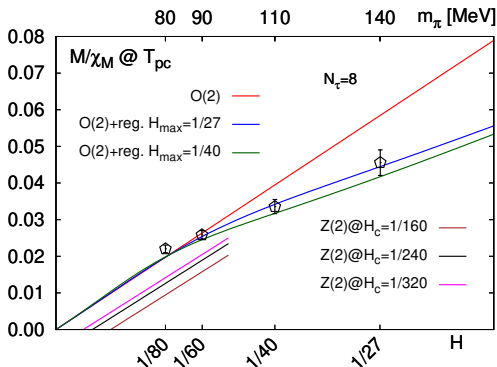
$H_{\max}^{-1}$	27	40
$T_c$ [MeV]	102(2)	95(3)
$\chi^2/\text{dof}$	3.58	2.68

# $M/\chi_M$ as a function of $H$ at $T_{pc}$



- $H\chi_M/M$  at  $T_{pc}$  is a constant given by the  $f_\chi(z_p)/f_G(z_p)$ , and it is almost volume independent. Regular terms are quadratic in  $tt_0$ .

# $M/\chi_M$ as a function of $H$ at $T_{pc}$



- ▶  $H\chi_M/M$  at  $T_{pc}$  is a constant given by the  $f_\chi(z_p)/f_G(z_p)$ , and it is almost volume independent. Regular terms are quadratic in  $tt_0$ .
- ▶ Non-vanishing critical pion mass can not describe the data.  
 $H_c = 1/320$  corresponds to a pion mass of 40 MeV in the continuum.

# Conclusions & Outlook

- ▶ We varied the quark mass range as well as the regular contribution in the finite size scaling fits to take care of the systematics. Fit parameters obtained from all the fits are combined to get a final value for  $T_c$  in the chiral limit,

$$T_c = 98_{-6}^{+3} \text{MeV.}$$

# Conclusions & Outlook

- ▶ We varied the quark mass range as well as the regular contribution in the finite size scaling fits to take care of the systematics. Fit parameters obtained from all the fits are combined to get a final value for  $T_c$  in the chiral limit,

$$T_c = 98_{-6}^{+3} \text{MeV.}$$

- ▶ In the explored pion mass range from 80 MeV to 140 MeV, no evidence of a first order phase transition was found.

# Conclusions & Outlook

- ▶ We varied the quark mass range as well as the regular contribution in the finite size scaling fits to take care of the systematics. Fit parameters obtained from all the fits are combined to get a final value for  $T_c$  in the chiral limit,

$$T_c = 98_{-6}^{+3} \text{MeV}.$$

- ▶ In the explored pion mass range from 80 MeV to 140 MeV, no evidence of a first order phase transition was found.
- ▶ Chiral observables at a finite lattice spacing show universal finite size scaling behavior which is consistent with the 3-d  $O(2)$  universality class.

# Conclusions & Outlook

- ▶ We varied the quark mass range as well as the regular contribution in the finite size scaling fits to take care of the systematics. Fit parameters obtained from all the fits are combined to get a final value for  $T_c$  in the chiral limit,

$$T_c = 98_{-6}^{+3} \text{MeV.}$$

- ▶ In the explored pion mass range from 80 MeV to 140 MeV, no evidence of a first order phase transition was found.
- ▶ Chiral observables at a finite lattice spacing show universal finite size scaling behavior which is consistent with the 3-d  $O(2)$  universality class.
- ▶ Next step would be to take the continuum limit. In doing so, careful consideration of the correct ordering of continuum limit and chiral limit is required. It is worthwhile to mention that in the (2+1)-flavor study, both these limits turned out to be interchangeable.